Nanoscale Res Lett (2010) 5:720–724
DOI 10.1007/s11671-010-9537-x

NANO EXPRESS

Stable Field Emitters for a Miniature X-ray Tube Using Carbon Nanotube Drop Drying on a Flat Metal Tip

Sung Hwan Heo · Aamir Ihsan · Seung Hwa Yoo · Ghafar Ali · Sung Oh Cho

Received: 7 December 2009 / Accepted: 8 January 2010 / Published online: 23 January 2010

Abstract Stable carbon nanotube (CNT) field emitters for a vacuum-sealed miniature X-ray tube have been fabricated. The field emitters with a uniform CNT coating are prepared by a simple drop drying of a CNT mixture solution that is composed of chemically modified multi-walled CNTs, silver nanoparticles, and isopropyl alcohol on flat tungsten tips. A highly thermal- and electrical-conductive silver layer strongly attaches CNTs to the tungsten tips. Consequently, the field emitters exhibit good electron emission stability: continuous electron emission of around 100 μA at 2.3 V/μm has stably lasted over 40 h even at non-high vacuum ambient ($\sim 10^{-3}$ Pa).

Keywords Carbon nanotube · Field emission · Drop drying · Miniature X-ray tube

Introduction

Carbon nanotube (CNT) as a cold field emitter emits high brightness of electron owing to their high aspect ratio, small radius of curvature, high electric and thermal conductivity, and structural robustness [1, 2]. Recently, CNT emitters have been intensively developed for electron sources of several devices, such as field emission displays (FED) [3–5], high-resolution X-ray microscopes [6–9], and miniature X-ray devices [10, 11]. A miniature X-ray tube [12–15] that normally consists of an electron emitter, an electron beam optical system, and an X-ray target has been applied to a cavity-inserted X-ray imaging [12] and a radiation source of brachytherapy for human body [13] with the help of its needle-like shape. However, since the inside of the tube is narrow and long, the electron emitter should be also miniaturized, and additional use of an electrostatic or magnetic lens for electron beam focusing is limited.

Recently, a thermionic filament-based miniature X-ray tube with the diameter of 2.25 mm and the dose rate of a 15 Gy/min (at 1 cm water depth) is commercialized for an X-ray source of electric brachytherapy [13, 14]. However, total operating time has been not guaranteed higher than 2.5 h. In such a thermionic filament-based X-ray tube, high temperature operation of the filament is necessary to increase X-ray dose rate, reducing the lifetime of the filament especially in non-high vacuum environment. CNT field emitters, particularly of a sharp tip shape, have been developed for high-resolution electron and X-ray devices [6, 7, 16–18]. CNT tip emitters can provide high-brightness electron beams due to their point-like electron emission sites. However, a sharp tip emitter has limited number of CNTs and thus each CNT must supply high electron emission current for the application to a high-power X-ray tube. As a result, CNTs can be easily damaged by high joule heating as well as ion particle adsorption [19]. In addition, an electron beam that is produced from a sharp tip is diverged because the electric field generated near the sharp exerts outward forces on the electrons generated from the tip. This diverged beam might be lost during the transport to an X-ray target in a miniature X-ray tube, which prevents the stable operation of the X-ray tube. One of the methods to overcome these properties of CNT tip emitters is to use a flat-tip CNTs, in which many CNTs are attached on a comparatively large area of flat metal substrate. In comparison with a sharp tip emitters, a flat-tip

S. H. Heo · A. Ihsan · S. H. Yoo · G. Ali · S. O. Cho (✉)
Department of Nuclear and Quantum Engineering, Korea Advanced Institute of Science and Technology (KAIST), 373-1 Guseong, Yuseong, Daejeon 305-701, Republic of Korea
e-mail: socho@kaist.ac.kr

CNT emitter reduces the electrical power loading per each CNT and can provide more parallel electron beam.

Generally, CNT field emitters have been fabricated using chemical vapor deposition (CVD) [6, 7, 20, 21], pyrolysis [22], screen printing of CNT paste [3, 4, 23], ion bombardment [24], and dielectrophoresis [25]. CVD techniques are appropriate for a precise control of CNT growth length, pattern, and direction [20]. However, in CVD method, a complicated process with high temperature is required, and moreover, the bonding strength of CNTs on a substrate depends on catalyst particle adhesion, which is generally not so strong. Ion bombardment and dielectrophoresis are comparatively simple processes, but the electron emission current of a CNT emitter fabricated by these technique is normally less than that prepared by CVD technique. In screen printing method, a mixture of CNT, inorganic binder, and solvent are printed on a substrate, and this method has the advantages of a simple and cheap process for mass production, stable and uniform electron emission with good CNT adhesion. In this method, an inorganic binder is sintered to form a high electric and thermal conductive layer [26] and tightly bonds CNTs to a substrate. Consequently, electron emitters prepared by this method have stable electron emission property for a longer time [23]. By adopting the advantage of the screen printing method, we fabricated a flat-tip CNT emitter for a miniature X-ray tube using drop drying of CNT solution [27, 28]. The fabricated CNT emitter has shown a high electron emission of $\sim$0.5 mA and a stable electron emission of 100 μA for longer than 40 h in the vacuum ambient of 1×10^{-3} Pa.

Experimental

The fabrication process of the CNT emitter is schematically shown in Fig. 1. The CNT solution has been prepared by mixing a multi-walled CNT (CM-95; Hanhwa Nanotech Inc.) with the diameter of 20 nm, silver (Ag) nanoparticles (NPs) (DGH; Advanced Nano Products Co., Ltd.) with the average diameter of $\sim$60 nm, and 99.5% isopropyl alcohol. The CNT has been synthesized by thermal CVD and purified using the hydrothermal treatment [29] with a mixture of nitric acid and sulfuric acid for a better CNT dispersion and cleaning adsorbates. The Ag NPs are filtered from the diluted Ag NP paste with isopropyl alcohol. The substrate of CNT is a tungsten (W) wire with the diameter of 0.25 mm. One end of the wire has been mechanically polished to have a flat surface with the average roughness of 0.1 μm in height and 0.4 μm in width for uniform coating of the CNT solution and regular electric field on the cathode tip surface. In Fig. 1a, 2 μl of the CNT solution drop dangles from the vertically stood W tip according to

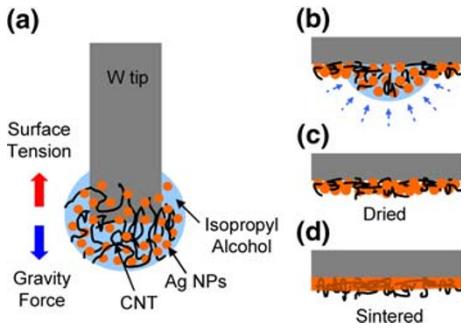

Fig. 1 Schematic diagrams of the CNT emitter fabrication. **a** The 2 μl of CNT mixture drop composed of multi-walled CNT, Ag nanoparticle (NP), and isopropyl alcohol hang down from a tungsten (W) tip end. **b**, **c** The CNT and Ag NP mixture are evaporated at the atmosphere to have uniform layer thickness. **d** The mixture layer is sintered in vacuum ambient $\sim 10^{-1}$ Pa at gradually increased temperature of 200°, 300°, 400°, 500°C for 30 min each

the force equilibrium between gravitational force and surface tension originated from the adhesion force between CNT solution and alcohol-philic metal substrate. During drying out of the isopropyl alcohol at atmosphere for 5 min, CNT and Ag NPs mixture is uniformly coated by evaporating sessile drop [30] (Fig. 1b, c). The sintering of the Ag NPs for good adhesion of CNT is processed in $\sim 10^{-1}$ Pa vacuum ambient at the gradually increased temperature of 200°, 300°, 400°, and 500°C for 30 min at each temperature (Fig. 1d). The concentration of CNT mixture was changed for a uniform coating of CNTs on a W tip. The fabricated emitters were analyzed by a scanning electron microscope (SEM; Hitachi S4800). Field emission properties were measured by using a diode structure at the base pressure of 1×10^{-3} Pa. The gap between a copper plate anode and the CNT emitter was 2.0 mm. Field emission current was continuously monitored by a precision current meter (Model: Fluke multimeter 189) and recorded at 10 min intervals.

Results and Discussion

The uniform coating of the CNT mixture on the metal-tip substrate follows the mechanisms of homogenization of CNT solution and the drop drying on alcohol-philic metal substrate. The chemically modified CNTs are not aggregated during the evaporation due to increased solubility in polar solvent by providing an oxygen-containing group on CNT surface [29]. Since the sessile drop is evaporated quasi-steadily [30], the CNT drop dried uniformly little by little from the outer diameter to the center of the metal tip through the reduction in air–alcohol interface [28] (decreasing contact angle/area). Figure 2 shows the scanning electron microscope (SEM) images of the dried CNT

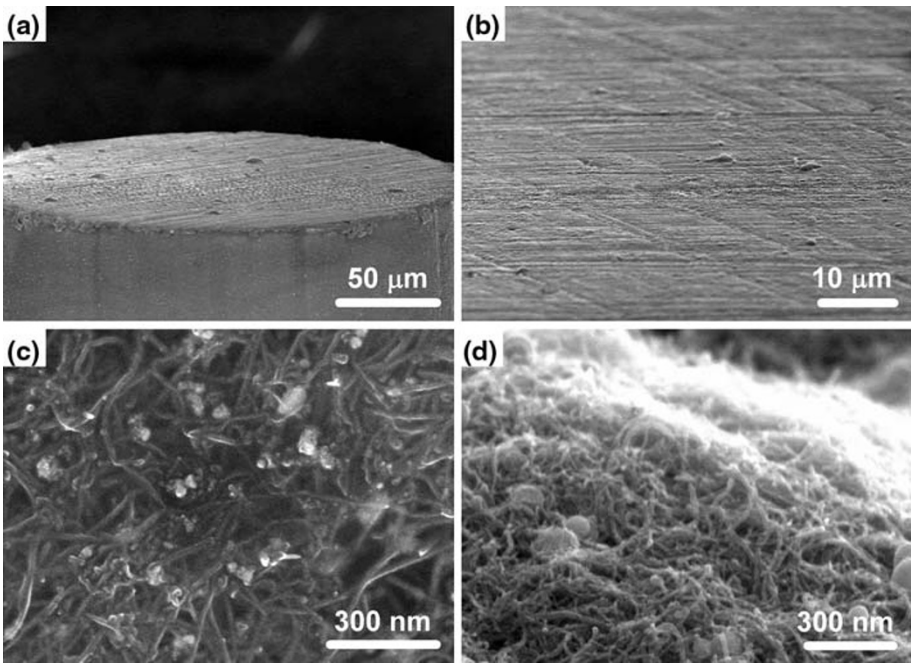

Fig. 2 SEM images of the fabricated CNT emitter. **a** The CNT mixture layer with the thickness of ~1.5 μm is adhered on the 0.25 mm diameter of the flat W tip surface by sintering. **b** The CNTs soared from the layer with height of ~0.5 μm and uniformly dispersed on the metal surface except few aggregations. **c** Drop dried pristine CNT-Ag NP mixture. **d** Sintered CNT-Ag NP mixture

drop morphology and the fabricated CNT emitter with 4.2 w% multi-walled CNT and 4.2 w% Ag NPs concentration. The CNT mixture layer with the thickness of ~1.5 μm hardened to the flat W tip after the sintering (Fig. 2a). The CNTs soared from the layer with height of ~0.5 μm and uniformly dispersed except few aggregations (Fig. 2b). The dried pristine and sintered CNT mixtures are shown in Fig. 2c, d. After sintering, most of the Ag NPs melted down, and few aggregated nanoparticles with the diameter of ~100 nm are remained on the CNT surface.

To optimize the uniform CNT coating, the concentration and mixing ratio of the CNT solution have been changed as shown in Fig. 3. In the Fig. 3a, b for the relatively higher concentration of Ag NPs, large amount of Ag particles are not homogeneously mixed with CNT and mutually aggregated as a protrusion on the CNT surface. However, in the

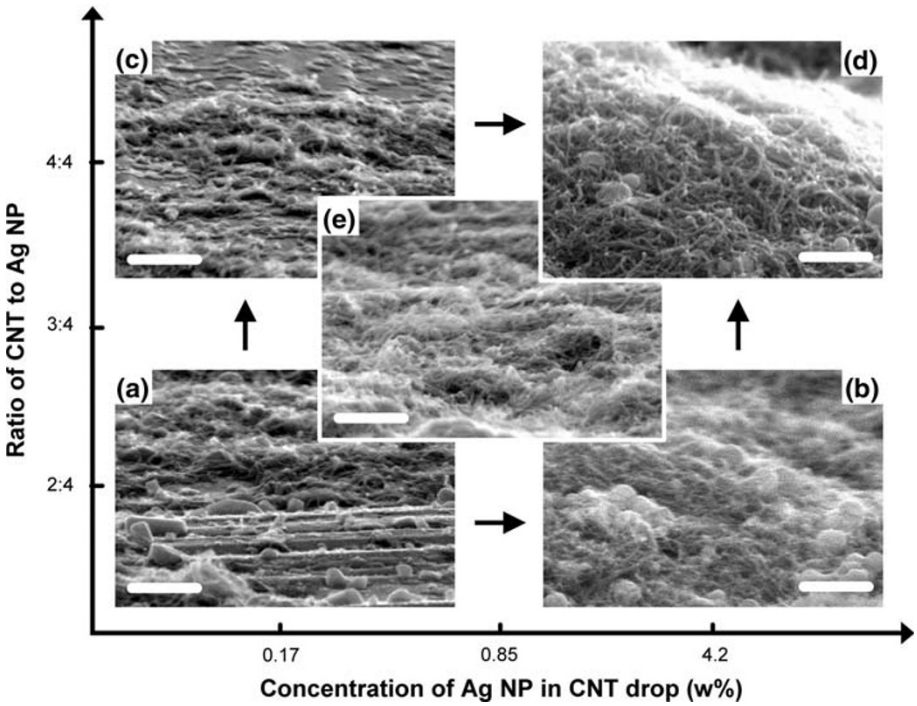

Fig. 3 SEM images of various CNT emitters fabricated by changing the ratio of CNT to Ag NP and the concentration of the mixture drop. The concentration of CNT and Ag NP in isopropyl alcohol is **a** 0.085 and 0.17 w%, **b** 2.1 and 4.2 w%, **c** 0.17 and 0.17 w%, **d** 4.2 and 4.2 w%, and **e** 0.64 and 0.85 w%. All *scale bars* represent 300 nm

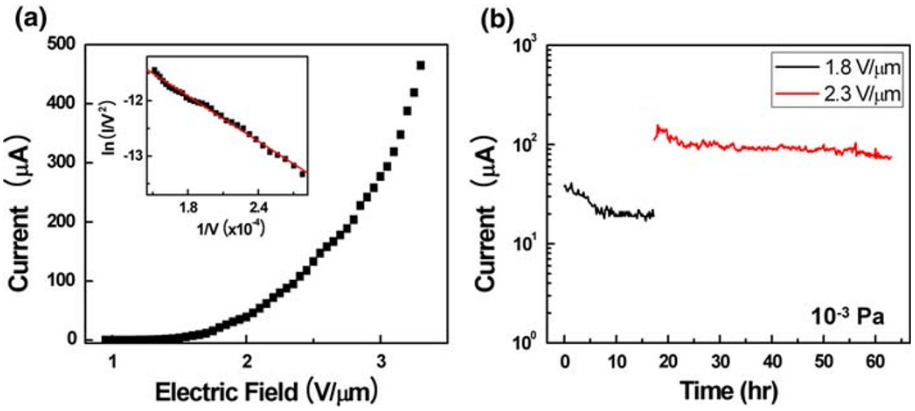

Fig. 4 Field emission properties of the fabricated CNT emitter. **a** Current in the ordinate is the emission current measured by increase in the electric field at anode. The inset is the FN plot of the emission current–voltage for the emitter. **b** The constant electric field mode field emission plot

Fig. 3c and d for the same concentration of CNT and Ag NPs, CNTs freely stand on the substrate without suppression of the residual Ag particles. The intermediate concentration of CNT mixture (Fig. 3e) shows that numbers of CNTs are aggregated with melted Ag layer, and therefore they do not stand up. The thickness of CNT mixture layer increased as ~0.1, ~0.4, and ~1.5 μm with increasing total concentration to 0.34, 1.7, and 8.4 w% for CNT/Ag NPs = 1/1, respectively. The sample shown in Fig. 3d has been tested for field emission owing to the relatively clean CNT surface and sufficient layer thickness for covering the roughness of the polished W tip surface.

Figure 4a displays the emission characteristics of the CNT emitter. The CNT emitter was pre-emitted at 1.8 V/μm for 17 h to clean the adsorbates on the CNT tip by the joule heating [31]. The threshold electric field for 10 mA/cm^2 was 1.55 V/μm and the electron current emitted over 465 μA at 3.3 V/μm. Emission area was estimated to be 4.9×10^{-4} cm^2, corresponding to the diameter of the W tip. The emission current–voltage curve well follows the Fowler–Nordheim (FN) equation [32]. The enhancement factor (β) [33] derived from FN plot [inset of Fig. 4a] was about 11,000. Figure 4b shows that the constant electric field mode field emission characteristics in 1×10^{-3} Pa vacuum ambient. In the first curve that presents self-cleaning of CNT emitter at 1.8 V/μm, the emission current degraded from 30 to 20 μA for 7 h during displacement of adsorbates and became stable within 2–3% until 17 h. After that, the electric field was increased to 2.3 V/μm for 100 μA. As shown in the second curve, the current shortly increased to 150 μA and degraded again to 100 μA at 17–21 h. 100 μA continued until 50 h with 3–4% current fluctuation and slowly decreased to 80 μA with the ratio of 0.04 μA/min until 58 h. After 58 h, a sudden change of the current was not occurred further, but the longer test is ongoing. The abrupt current increase in the second curve might be related to an imperfect CNT adhesion on Ag layer. Some of the CNT layer might be broken off by joule heating induced high temperature, and consequently parts of the CNT stand up to emit more electrons until the loss of adhesion. The slow current decrease is strongly related to the structure deformation of CNTs from a crystalline nanotube to an amorphous carbon fiber due to the

Table 1 Field emission properties of the various CNT emitters on sharp substrates

Substrate	Production method	Emission area (cm^2)	Best emission	Vacuum ambient (Pa)	Stability	Refs.
Conical tip	Plasma-enhanced CVD	1.6×10^{-6}	26 μA, 1.2 kV/250 μm	4×10^{-7}	10 μA, >20 h	[6]
	Inductively coupled plasma CVD	$\sim 3 \times 10^{-8}$ (1 μm end diameter)	51 μA, 1 kV/250 μm	1.06×10^{-5}	10 μA, >40 h	[16]
	Pyrolysis of ferrocene	6.7×10^{-7}	1 mA, 16.5 kV/5 cm	1×10^{-8}	100 μA, >180 min	[17]
	Plasma-enhanced CVD	1.2×10^{-9}	~100 μA, 2.7 kV/1 mm	1×10^{-8}	80 μA, >100 h	[18]
Wire	Arc	$\sim 5.9 \times 10^{-4}$ (125 μm ϕ, 0.3 mm length)	7 mA/cm^2, 6 kV/1 mm	2.6×10^{-4}	2 mA/cm^2, >15 h	[34]
	Plasma-enhanced CVD	$\sim 7.9 \times 10^{-4}$ (50 μm ϕ, 1 mm length)	1 mA, 4.3 V/1 mm	1×10^{-9}	1 mA, >5,000 h	[35]
Flat plate	Arc/Ag paste	2×10^{-2}	10 mA/cm^2, 2.2 V/μm	$\sim 1 \times 10^{-6}$	~210 μA, >8,000 h	[36]
	Printed CNT	2.83	8 mA, 1.55 kV/0.5 mm	$\sim 1.3 \times 10^{-5}$	~0.6 mA, >100 h	[4]
	CVD	5.6×10^{-3}	100 mA/cm^2, 12 kV/1 mm	$\sim 1.3 \times 10^{-5}$	~300 μA, >15 h	[8]
Flat tip	CVD/Ag NP paste	4.9×10^{-4}	465 μA, 6.6 kV/2 mm	$\sim 1 \times 10^{-3}$	~100 μA, >40 h	

migration of positively charged residual gas particles toward negatively charged CNT emitter and joule heating [19]. The flat-tip-type CNT emitter fabricated with the Ag adhesion layer can provide larger number of CNTs for electron emission, and thus the electric power loading per CNT is decreased. Table 1 shows the field emission properties of various CNT emitters fabricated on sharp substrates, which are recently published [4, 6, 8, 16, 17, 34–36]. The flat-tip substrate can provide an enough electron emission site for high emission current similar to that of a flat plate, and together with the CNT mixture coating can help to stabilize electron emission in a worse vacuum condition. In addition, with the flat-tip substrate, the structural damage to the CNT tips due to ionic collisions will be less likely to occur. Therefore, a fatal emission failure in a bad vacuum condition has been lessened compared to sharp-tip-type CNT emitters [6, 16, 17].

Conclusions

In summary, flat-tip-type CNT field emitters were fabricated by drop drying of a CNT-Ag NP mixture on flat tungsten tips. We observed that the concentration and mixing ratio of the CNT solution were crucial for the performance of CNT field emitters. The fabricated tip-type field emitters exhibited very stable electron emission at high emission current. We believe that the tip-type CNT field emitters are very useful to realize a miniaturized X-ray tube with a high X-ray brightness.

Acknowledgments This work was supported by the Korea Science and Engineering Foundation (KOSEF) grant funded by the Korea Ministry of Education, Science and Technology (MEST) (No. 2009-0081819).

References

1. S. Iijima, Nature (Lond.) **354**, 56 (1991)
2. N. de Jonge, Y. Lamy, K. Schoots, T.H. Oosterkamp, Nature **420**, 393 (2002)
3. M.S. Jung, J.H. Lee, J.H. Lee, J.J. Park, I.S. Jung, J.M. Kim, Adv. Funct. Mater. **18**, 449 (2008)
4. Y.C. Kim, J.W. Nam, M.I. Hwang, I.H. Kim, C.S. Lee, Y.C. Choi, J.H. Park, H.S. Kim, J.M. Kim, Appl. Phys. Lett. **92**, 263112 (2008)
5. W.B. Choi, D.S. Chung, J.H. Kang, H.Y. Kim, Y.W. Jin, I.T. Han, Y.H. Lee, J.E. Jung, N.S. Lee, G.S. Park, J.M. Kim, Appl. Phys. Lett. **75**, 3129 (1999)
6. S.H. Heo, A. Ihsan, S.O. Cho, Appl. Phys. Lett. **90**, 183109 (2007)
7. Y. Sakai, A. Haga, S. Sugita, S. Kita, S.-I. Tanaka, F. Okuyama, N. Kobayashi, Rev. Sci. Instrum. **78**, 013305 (2007)
8. Z. Liu, G. Yang, Y.Z. Lee, D. Bordelon, J. Lu, O. Zhou, Appl. Phys. Lett. **89**, 103111 (2006)
9. R. Yabushita, K. Hata, Surf. Interface Anal. **40**, 1664 (2008)
10. A. Haga, S. Senda, Y. Sakai, Y. Mizuta, S. Kita, F. Okuyama, Appl. Phys. Lett. **84**, 2208 (2004). **84**, 5046 (2004)
11. S. Senda, Y. Sakai, Y. Mizuta, S. Kita, F. Okuyama, Appl. Phys. Lett. **85**, 5679 (2004)
12. K. Dickmann, C. Fotakis, J.F. Asmus, *Lasers in the conservation of artworks*, vol. 100 (Springer, Berlin Heidelberg, 2005), pp. 353–356
13. D. Liu, E. Poon, M. Bazalova, B. Reniers, M. Evans, T. Rusch, F. Verhaegen, Phys. Med. Biol. **53**, 61 (2008)
14. A. Dickler, Nat. Clin. Pract. Oncol. **6**, 138 (2009)
15. C. Ribbing, N. Strid, P. Rangsten, J. Tiren, Biomed. Microdev. **4**, 285 (2002)
16. J.P. Kim, Y.K. Kim, C.K. Park, H.Y. Choi, C.H. Shon, J.U. Kim, J.S. Park, Diam. Relat. Mater. **18**, 486 (2009)
17. R.B. Sharma, V.N. Tondare, D.S. Joag, A. Govindaraj, C.N.R. Rao, Chem. Phys. Lett. **344**, 283 (2001)
18. Y. Sakai, D. Tone, S. Nagatsu, T. Endo, S. Kita, F. Okuyama, Appl. Phys. Lett. **95**, 073104 (2009)
19. J.H. Lee, S.H. Lee, W.S. Kim, H.J. Lee, J.N. Heo, T.W. Jeong, C.W. Baik, S.H. Park, S. Yu et al., Appl. Phys. Lett. **89**, 253115 (2006)
20. Y. Chen, D.T. Shaw, L. Guo, Appl. Phys. Lett. **76**, 2469 (2000)
21. S.K. Srivastava, V.D. Vankar, V. Kumar, Nanoscale Res. Lett. **3**, 25 (2008)
22. I. Kunadian, R. Andrews, D. Qian, M.P. Menguc, Carbon **47**, 384 (2009)
23. X.X. Zhang, C.C. Zhu, Microelect. J. **40**, 1166 (2009)
24. T.T. Tan, H.S. Sim, S.P. Lau, H.Y. Yang, M. Tanemura, J. Tanaka, Appl. Phys. Lett. **88**, 103105 (2006)
25. J. Zhang, J. Tang, G. Yang, Q. Qiu, L.C. Qin, O. Zhou, Adv. Mater. **16**, 1219 (2004)
26. K.S. Moon, H. Dong, R. Maric, S. Pothukuchi, A. Hunt, Y. Li, C.P. Wong, J. Electron. Mater. **34**, 168 (2005)
27. R. Duggal, F. Hussian, M. Pasquali, Adv. Mater. **18**, 29 (2006)
28. W.R. Small, C.D. Walton, J. Loos, M. in het Panhuis, J. Phys. Chem. B **110**, 13029 (2006)
29. V. Datsyuk, M. Kalyva, K. Papagelis, J. Parthenios, D. Tasis, A. Siokou, I. Kallitsis, C. Galiotis, Carbon **46**, 833 (2008)
30. H. Hu, R.G. Larson, J. Phys. Chem. B **106**, 1334 (2002)
31. S.T. Purcell, P. Vincent, C. Journet, V.T. Binh, Phys. Rev. Lett. **88**, 105502 (2002)
32. R.H. Fowler, L.W. Nordheim, Proc. R. Soc. Lond. Ser. A **119**, 173 (1928)
33. J.M. Bonard, H. Kind, T. Stockli, L.O. Nilsson, Solid State Electron. **45**, 893 (2001)
34. Y.B. Zhang, S.P.L. Huang, M. Tanemura, Appl. Phys. Lett. **86**, 123115 (2005)
35. S. Kita, Y. Watanabe, A. Ogawa, K. Ogura, Y. Sakai, Y. Matsumoto, Y. Isokane, F. Okuyama, T. Nakazato, T. Otsuka, J. Appl. Phys. **103**, 064505 (2008)
36. Y. Saito, S. Uemura, Carbon **38**, 169 (2000)